

Radial Electric Field Control for Retardation of Radial Transport of Bounce Ions in the Tandem Mirror

ISHII Kameo, TAKEMURA Yuichiro, KOJIMA Atsushi, HAGISAWA Kazuhisa,
MIYATA Yoshiaki, KATANUMA Isao and CHO Teruji

Plasma Research Center, University of Tsukuba, Ibaraki 305-8577, Japan

(Received: 9 December 2003 / Accepted: 26 June 2004)

Abstract

Existence of the bounced ions by the plug potential is essential in order to improve the confinement in the tandem mirror. The anchor cell with non-axisymmetric magnetic field configuration is installed between the plug/barrier cell and the central cell to stabilize the magnetohydrodynamics (MHD) instability. The electro-statically trapped ions are bounced at the plug region after passing through the anchor cell from the central cell. The trajectories of the bounce ions are calculated on the assumption that the cross-sectional shape of the magnetic flux tube is slightly different from the cross-sectional shape of the equi-potential surface at the mirror throats of the anchor cell. Radial drift is estimated as a function of the discrepancy of the shapes. It is pointed out that control of the radial electric field is effective to retard the radial transport.

Keywords:

radial electric field, bounce ion, trajectory, radial transport, tandem mirror

1. Introduction

In the tandem mirror, axial confinement has been improved by electrostatic potentials created on both sides of the plasma [1,2,3]. The hyperboloidal loss boundaries in the velocity space were shifted in the direction of the higher energy side along a velocity component axis parallel to the magnetic field so as to decrease the inflow of plasma into the loss region from the trapped region caused by the Coulomb collision. We confirmed, from a microscopic point of view, the confining potential created by the microwave injection, that is, from observation of the velocity distribution function of the end-loss ions [4]. As a subsequent subject of the improvement of the axial confinement due to the potential plugging, radial transport across the magnetic field has attracted interest recently. The radial transport across the magnetic field seems to be induced mainly at the anchor cell having a non-axisymmetric magnetic field configuration and at the plug/barrier cell with a potential hill and a potential dip, and the ion diffusion across the loss boundary seems to be enhanced by fluctuations excited in the plasma [5].

Investigation of the radial transport of ions bouncing between magnetic mirrors or electrostatic potentials is useful for the optimization of the radial potential profile to improve the tandem mirror experiment. Here we calculated the ion trajectories using a direct method and the guiding center approximation, and paid attention to the radial transport of the bounced ions by the plug potential caused by the

discrepancy of the shapes between the magnetic flux tube and the equi-potential surface at the mirror regions of the anchor cell.

2. Magnetic field configuration of the tandem mirror

Two anchor cells with a minimum B magnetic configuration are located on both sides of an axisymmetric central solenoid through the re-circularizing regions in the tandem mirror GAMMA 10, and two axisymmetric plug/barrier cells are connected to the anchor cells as the outboard thermal barrier configuration in order to remove the resonance diffusion [3]. The cross section of the magnetic flux tube is well approximated by an ellipse, and at the mirror throat of the anchor cell the eccentricity $\sqrt{1 - b_c^2/a_c^2}$ of the ellipse is estimated to be 0.999819, where a_c and b_c are a major axis and a minor axis of the ellipse, respectively. The magnetic coils and the magnetic field lines are shown together with the locations of the heating systems in Fig. 1 (a), and the axial profiles of the magnetic field strength and the schematic electrostatic potential are shown in Fig. 1 (b). In order to produce the main plasma and heat the ions, ion-cyclotron range of frequency (ICRF) waves are injected into the target plasma in the central cell, which is produced along the magnetic field line from both ends of the machine. The magnetic field strength is almost the same and the strongest

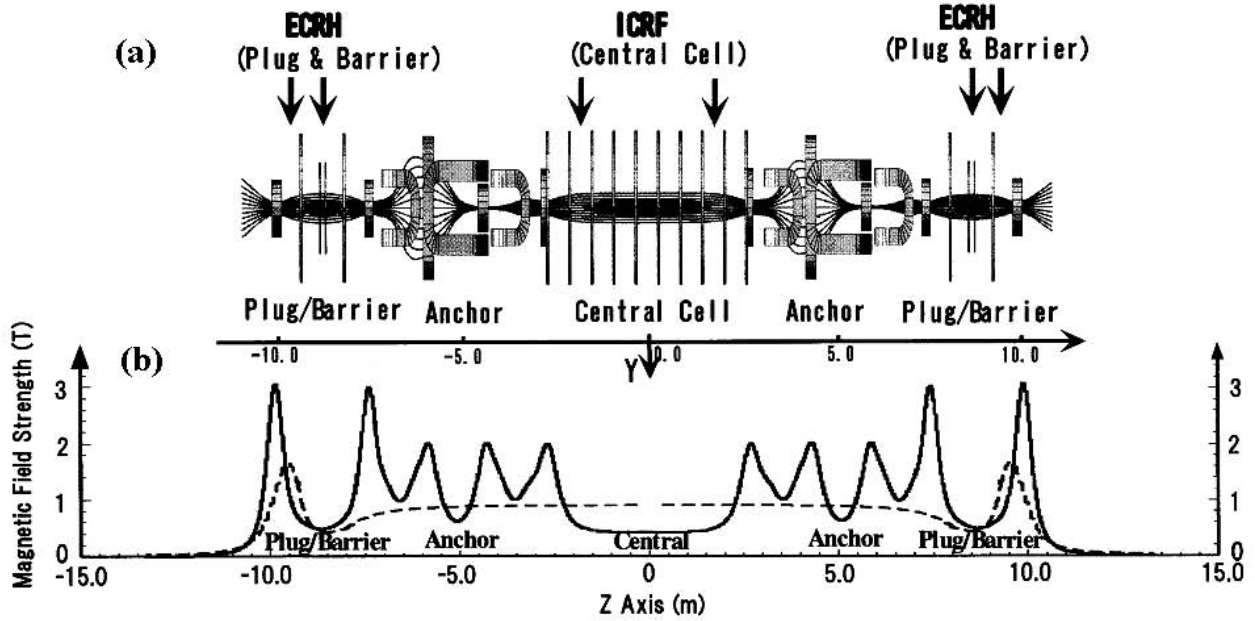


Fig. 1 (a) Locations of the heating systems.
(b) A dotted line shows a schematic axial profile of the potential.

(~30 kG) at both inner mirror throat (IMT) and outer mirror throat (OMT) of the plug/barrier cell. Two microwaves are injected into the plug region (~10 kG) and the thermal barrier region (~5 kG) of the plug/barrier cell in order to create the plug potential and the thermal barrier potential by carrying out electron-cyclotron resonance heating (ECRH), respectively. Coaxially separated end plates divided into 5 areas are installed in front of the end walls of the vacuum vessel in order to control the radial potential profile of the core plasma.

3. Bounce ions

3.1 Ion bounce region

The bounce ions are shown schematically in Fig. 2 (a) with axial profiles of the magnetic field strength and the electrostatic potential. Some of the ions that have passed through the mirror throats of the central and anchor cells from the central cell are reflected in front of the IMT due to the magnetic mirror effect, and some residual ions with lower energy than the confining potential and with small pitch angles, which passed through the IMT, are reflected near the plug region due to the potential hill. A portion of the ions having high energy is reflected in the neighborhood of the OMT after passing over the plug potential hill. Here, we define these ions as an IMT bounce ion, a plug potential (PP) bounce ion and an OMT bounce ion, respectively. Figure 2 (b) shows, as an example, the end-loss region and the bounce regions in which the IMT, PP and OMT bounce ions occupy in the $\epsilon - \mu$ space, where ϵ and μ are the ion total energy and the magnetic moment, respectively. The loss region is surrounded with the PP bounce region and the OMT bounce region in this case, and therefore the ions trapped in the tandem mirror flow mainly into the loss region via the PP

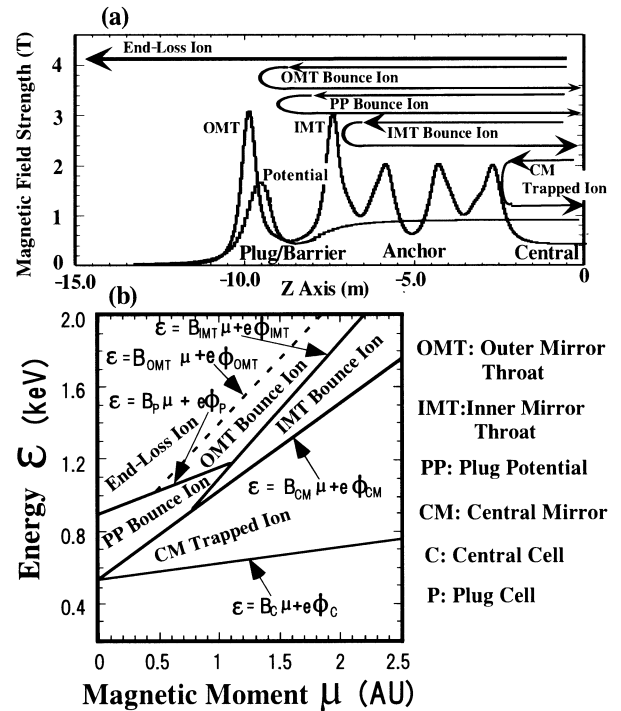


Fig. 2 (a) Bounce ions and axial profiles of the magnetic field strength and electrostatic potential.
(b) Bounce ion regions in the $\epsilon - \mu$ space.

and OMT bounce regions. In the case that the machine transit time of the trapped ions in the PP and OMT bounce regions is much shorter than the deflection time, the ions go to the end wall as end-loss ions after several bouncing.

3.2 Trajectories of bounce ions

The anchor cells are installed between the central cell

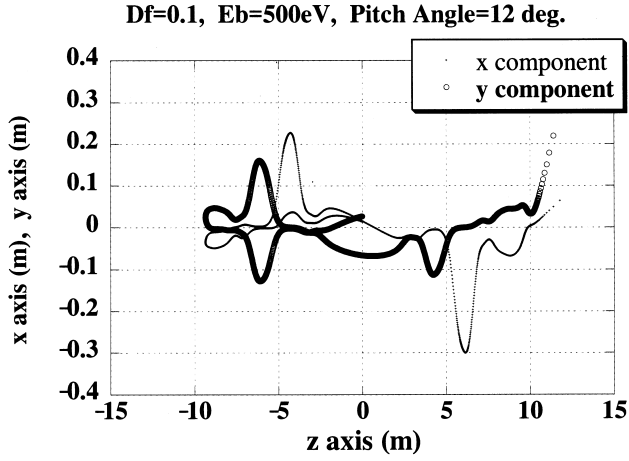


Fig. 3 The initial ion was emitted from the position of a radius 0.03 m on the mid-plane of the central cell. The trapped ion was changed to the end-loss ion.

and the plug/barrier cells in order to stabilize the MHD instability. The eccentricity of the elliptic cross section of the magnetic flux tube is 0.999819 at the mirror throat of the anchor cell. It seems that in the case of high radial electric field the electrostatic potential is not perfectly constant along the magnetic field line through the anchor cells between the IMTs of both plug/barrier cells and the equi-potential surface slightly deforms due to the slight deviation from equilibrium state.

On the assumption that the shape of the magnetic flux tube did not necessarily coincide with the equi-potential surface, we calculated, as an example of radial drift, the trajectories of the ions that started from the mid-plane of the central cell. The point to which special attention should be paid is the radial drift of the bounce ions due to the discrepancy of the curvatures in the major axis region of the elliptic cross section at the mirror throat areas of the anchor cells between the magnetic flux tube and the equi-potential surface. We assumed that the radial potential profile $\phi(r)$ was axi-symmetric and Gaussian on the mid-plane ($z = 0$ m) of the central cell and that the central potential was 300 V, the barrier potential was 0 V and the plug potential was 1,500 V, that is, the thermal barrier depth was 300 V and the confinement potential was 1,200 V. $\phi(r) = \phi_0(0)\exp[-(\ln(2)/r_h(0)^2)r^2]$, where $\phi_0(0)$ is the potential at $z = 0$ m and $r = 0$ m and equals to 300 V, r is a radial coordinate at $z = 0$ m and $r_h(0) = 0.07$ m. As the cross section of the magnetic flux tube was well approximated by an ellipse, we assumed, as a generalized radial potential profile, that the radial potential profile had two Gaussian types of components in the directions of the x and y axes. That is, $\phi_x(r_x(z)) = \phi_0(z)\exp[-(\ln(2)/r_{xh}(z)^2)r_x(z)^2]$, $\phi_y(r_y(z)) = \phi_0(z)\exp[-(\ln(2)/r_{yh}(z)^2)r_y(z)^2]$, where $r_{xh}(z) = r_{xhf}(z) - [r_{xhf}(z) - r_h(0)]D_f$ and $r_{yh}(z) = r_{yhf}(z) - [r_{yhf}(z) - r_h(0)]D_f$, $2r_{xh}(z)$ and $2r_{yh}(z)$ are the full width at half maximum (FWHM) for each potential profile at the coordinate z , $r_{xhf}(z)$ and $r_{yhf}(z)$ are distances of the magnetic field lines from the z axis, which pass through

Ion Energy : 0.5 keV
FWHM(Potential) : 0.08 (m)

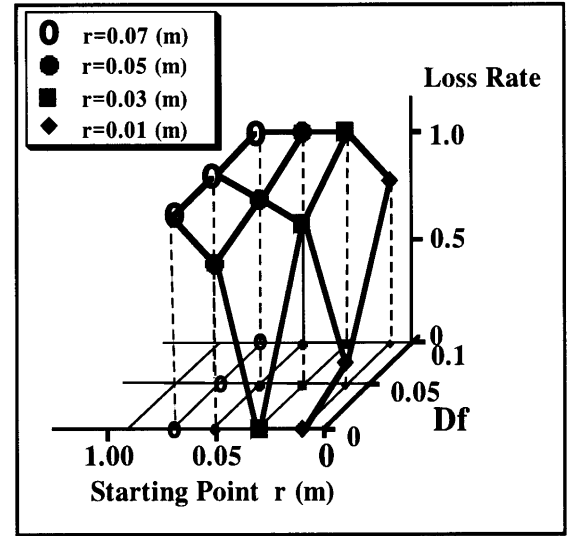


Fig. 4 The loss rate was estimated as a function of the starting position and the deformation factor.

the points of xyz coordinates (0.07, 0, 0) and (0, 0.07, 0), respectively, and D_f is defined as a deformation factor. In the case of $D_f = 0$, the equi-potential surface coincides perfectly with the magnetic flux tube. We directly calculated the trajectories of the plug potential bounce ions moving under the influence of the magnetic field and the above electric field, and found the effect of the deformed radial potential profile on the radial drift as a function of the deformation factor D_f .

The trajectories of 9 ions were calculated, which started from the mid-plane of the central cell with pitch angles of 12° , 16° , 20° on the condition of $D_f = 0.0, 0.05, 0.1$ and 0.2 . The initial 9 ions were placed at regular intervals on semicircles with radiuses of 0.01, 0.03, 0.05, 0.07, 0.09 m, located on the mid-plane of the central cell, and were emitted with energies of 0.5 keV and 1.0 keV. As the loss cone angle is 21.2° , all ions with pitch angle of 12° will be reflected in front of the plug potential after passing through the IMT region. Figure 3 shows, as an example, the projected trajectories of the transferred ions from the trapped region to the loss region.

4. Radial transport of ions

Three types of Gaussian potential profiles were used with the FWHM of 0.08 m, 0.14 m and 0.28 m at the central cell. The profiles have the maximum electric field of $\sim 5,000$, $\sim 3,000$ and $\sim 1,500$ V/m, respectively. We estimated the loss rate of the ions changed to end-loss ions during one reciprocation to the initially trapped ions by the confining potential as a function of the deformation factor and the radius of the starting circle of the ion position as shown in Fig. 4. The calculated results indicated that the radial drift was not effective for the ions moving under the influence of the $\vec{E} \times \vec{B}$ drift in the case of $D_f = 0.0$, and the radial drift

depended on the increase of the deformation factor and also strongly on the radial electric field. The radial drift was enhanced even in $D_f = 0.05$ which corresponded to the decrease of 0.07% in the eccentricity of the cross section. Increase of the area of the core plasma with the flattened radial electric field, which is confined by the electrostatic potential, is quite effective for preventing the plug potential bounce ion from flowing into the loss region and sustaining the bounce ions.

5. Conclusions

The trajectories of the bounced ions by the plug potential were calculated on the assumption that the shape of the magnetic flux tube was slightly different from the shape of the equi-potential surface at the mirror throats of the anchor cell with the non-axisymmetric magnetic field configuration. The discrepancy enhances the radial transport for the bounce

ions to flow from the bounce region to the loss region. It is effective to increase the area of the core plasma with the flattened radial electric field for improvement of the confinement, and therefore the microwave injection for the creation of the plug potential should be considered from this point of view.

References

- [1] G.I. Dimov, V.V. Zakaidakov and M.E. Kishinevskii, *Sov. J. Plasma Phys.* **2**, 326 (1976).
- [2] T.K. Fower and B.G. Logan, *Comments Plasma Phys. Controll. Fusion* **2**, 167 (1977).
- [3] M. Inutake *et al.*, in *Proceedings of the 3rd Technical Committee Meeting and Workshop* (IAEA, Tokyo, 1983) Vol. 1, p. 429 (Report No. IAEA-TC-392/25, 1983).
- [4] K. Ishii *et al.*, *Phys. Fluids B* **4**, No. 12, 3823 (1992).
- [5] K. Ishii *et al.*, *J. Plasma Fusion Res.* **78**, 1239 (2002).